

Two-pion contributions to the muon $g - 2$

Peter Stoffer

Physics Department, UC San Diego

in collaboration with G. Colangelo and M. Hoferichter

arXiv:1810.00007 [hep-ph], submitted to JHEP

and with G. Colangelo, M. Hoferichter, and M. Procura

JHEP **04** (2017) 161, [arXiv:1702.07347 [hep-ph]]

Phys. Rev. Lett. **118** (2017) 232001, [arXiv:1701.06554 [hep-ph]]

JHEP **09** (2015) 074, [arXiv:1506.01386 [hep-ph]]

JHEP **09** (2014) 091, [arXiv:1402.7081 [hep-ph]]

and work in progress

2nd December 2018

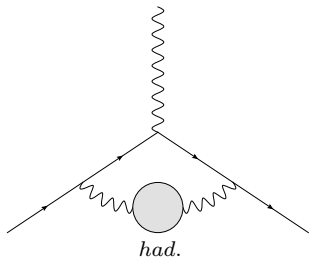
SchwingerFest 2018

Mani L. Bhaumik Institute, UCLA

- 1 Hadronic contributions to the muon $g - 2$
- 2 Hadronic vacuum polarisation
 - Dispersion relation for the pion vector form factor
 - Fit strategy
 - Fit results and contribution to the muon $g - 2$
- 3 Hadronic light-by-light scattering
 - Tensor decomposition and Mandelstam representation
 - Pion pole
 - Pion box
 - $\pi\pi$ -rescattering
- 4 Conclusions and outlook

- 1 Hadronic contributions to the muon $g - 2$
- 2 Hadronic vacuum polarisation
- 3 Hadronic light-by-light scattering
- 4 Conclusions and outlook

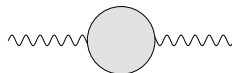
Hadronic vacuum polarisation (HVP)



- problem: QCD is non-perturbative at low energies
- much progress using lattice QCD first-principle calculations
- best current evaluations based on dispersion relations and data (or combinations with lattice)

Hadronic vacuum polarisation (HVP)

Photon HVP function:



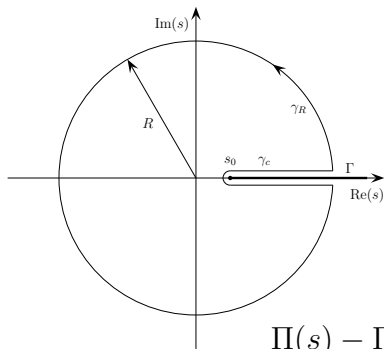
$$\text{wavy line} \text{---} \text{circle} \text{---} \text{wavy line} = i(q^2 g_{\mu\nu} - q_\mu q_\nu) \Pi(q^2)$$

Unitarity of the S -matrix implies the optical theorem:

$$\text{Im}\Pi(s) = \frac{s}{e(s)^2} \sigma(e^+ e^- \rightarrow \text{hadrons})$$

Dispersion relation

Causality implies analyticity:



Cauchy integral formula:

$$\Pi(s) = \frac{1}{2\pi i} \oint_{\gamma} \frac{\Pi(s')}{s' - s} ds'$$

Deform integration path:

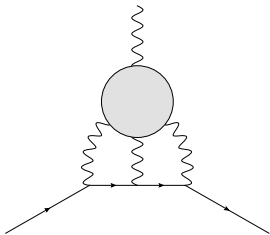
$$\Pi(s) - \Pi(0) = \frac{s}{\pi} \int_{4M_{\pi}^2}^{\infty} \frac{\text{Im}\Pi(s')}{(s' - s - i\epsilon)s'} ds'$$

HVP contribution to $(g - 2)_\mu$

$$a_\mu^{\text{HVP}} = \frac{m_\mu^2}{12\pi^3} \int_{s_{\text{thr}}}^{\infty} ds \frac{\hat{K}(s)}{s} \sigma(e^+e^- \rightarrow \text{hadrons})$$

- basic principles: unitarity and analyticity
- direct relation to experiment: total hadronic cross section $\sigma(e^+e^- \rightarrow \text{hadrons})$
- can be systematically improved: dedicated e^+e^- program (BaBar, Belle, BESIII, CMD3, KLOE2, SND)

Hadronic light-by-light (HLbL) scattering



- so far only model calculations
- uncertainty estimate based rather on consensus than on a systematic method
- with recent progress on vacuum polarisation, HLbL starts to dominate the theory uncertainty
- progress with lattice QCD and dispersive approach

① Hadronic contributions to the muon $g - 2$

SM contributions to $(g - 2)_\mu$

	$10^{11} \times a_\mu$	$10^{11} \times \Delta a_\mu$	
BNL E821	116 592 089	63	→ PDG 2016
QED total	116 584 718.97	0.07	→ Aoyama et al. 2012, 2017
EW	153.6	1.0	→ Gnendiger et al. 2013
LO HVP	6 932.7	24.6	→ Keshavarzi et al. 2018
NLO HVP	-98.2	0.4	→ Keshavarzi et al. 2018
NNLO HVP	12.4	0.1	→ Kurz et al. 2014
LO HLbL	102	39	→ Nyffeler 2017
NLO HLbL	3	2	→ Colangelo et al. 2014
Hadronic total	6952	46	
Theory total	116 591 825	46	

① Hadronic contributions to the muon $g - 2$

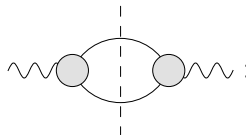
SM contributions to $(g - 2)_\mu$

	$10^{11} \times a_\mu$	$10^{11} \times \Delta a_\mu$	
BNL E821	116 592 089	63	→ PDG 2016
QED total	116 584 718.97	0.07	→ Aoyama et al. 2012, 2017
EW	153.6	1.0	→ Gnendiger et al. 2013
LO HVP	6 931	34	→ Davier et al. 2017
NLO HVP	-98.2	0.4	→ Keshavarzi et al. 2018
NNLO HVP	12.4	0.1	→ Kurz et al. 2014
LO HLbL	102	39	→ Nyffeler 2017
NLO HLbL	3	2	→ Colangelo et al. 2014
Hadronic total	6950	52	
Theory total	116 591 823	52	

- 1 Hadronic contributions to the muon $g - 2$
- 2 Hadronic vacuum polarisation**
 - Dispersion relation for the pion vector form factor
 - Fit strategy
 - Fit results and contribution to the muon $g - 2$
- 3 Hadronic light-by-light scattering
- 4 Conclusions and outlook

Two-pion contribution to HVP

- $\pi\pi$ contribution amounts to more than 70% of HVP contribution
- responsible for a similar fraction of HVP uncertainty
- unitarity relation for $\pi\pi$ contribution to HVP: pion vector form factor (VFF)



$\sigma(e^+e^- \rightarrow \pi^+\pi^-) \propto |F_\pi^V(s)|^2$

Two-pion contribution to HVP

- VFF itself fulfils again a unitarity relation:

$$\text{Diagram} = \text{Diagram}_1 + \text{Diagram}_2 + \dots$$

- use the constraints of analyticity and unitarity to better understand uncertainties in HVP $\pi\pi$ channel

→ de Trocóniz, Ynduráin, 2001, 2004; Leutwyler, Colangelo 2002, 2003;

Ananthanarayan et al. 2013, 2016

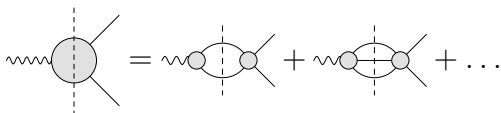
Dispersive representation of pion VFF

$$F_{\pi}^V(s) = \Omega_1^1(s) \times G_{\omega}(s) \times G_{\text{in}}^N(s)$$

- Omnès function with elastic $\pi\pi$ -scattering P -wave phase shift $\delta_1^1(s)$ as input:

$$\Omega_1^1(s) = \exp \left\{ \frac{s}{\pi} \int_{4M_{\pi}^2}^{\infty} ds' \frac{\delta_1^1(s')}{s'(s' - s)} \right\}$$

Dispersive representation of pion VFF



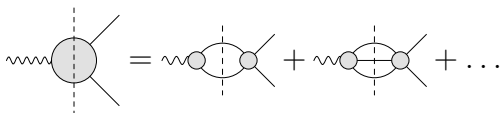
$$F_{\pi}^V(s) = \Omega_1^1(s) \times G_{\omega}(s) \times G_{\text{in}}^N(s)$$

- isospin-breaking 3π intermediate state: negligible apart from ω resonance ($\rho - \omega$ interference effect)

$$G_{\omega}(s) = 1 + \frac{s}{\pi} \int_{9M_{\pi}^2}^{\infty} ds' \frac{\text{Im}g_{\omega}(s')}{s'(s'-s)} \left(\frac{1 - \frac{9M_{\pi}^2}{s'}}{1 - \frac{9M_{\pi}^2}{M_{\omega}^2}} \right)^4,$$

$$g_{\omega}(s) = 1 + \epsilon_{\omega} \frac{s}{(M_{\omega} - \frac{i}{2}\Gamma_{\omega})^2 - s}$$

Dispersive representation of pion VFF



$$F_{\pi}^V(s) = \Omega_1^1(s) \times G_{\omega}(s) \times G_{\text{in}}^N(s)$$

- heavier intermediate states: 4π (mainly $\pi^0\omega$), $\bar{K}K$, ...
- described in terms of a conformal polynomial with cut starting at $\pi^0\omega$ threshold

$$G_{\text{in}}^N(s) = 1 + \sum_{k=1}^N c_k (z^k(s) - z^k(0))$$

- correct P -wave threshold behaviour imposed

Input and systematic uncertainties

- elastic $\pi\pi$ -scattering P -wave phase shift $\delta_1^1(s)$ from Roy-equation analysis, including uncertainties
→ [Ananthanarayan et al., 2001](#); [Caprini et al., 2012](#)
- high-energy continuation of phase shift above validity of Roy equations
- ω width
- systematics in conformal polynomial: order N , one mapping parameter

Free fit parameters

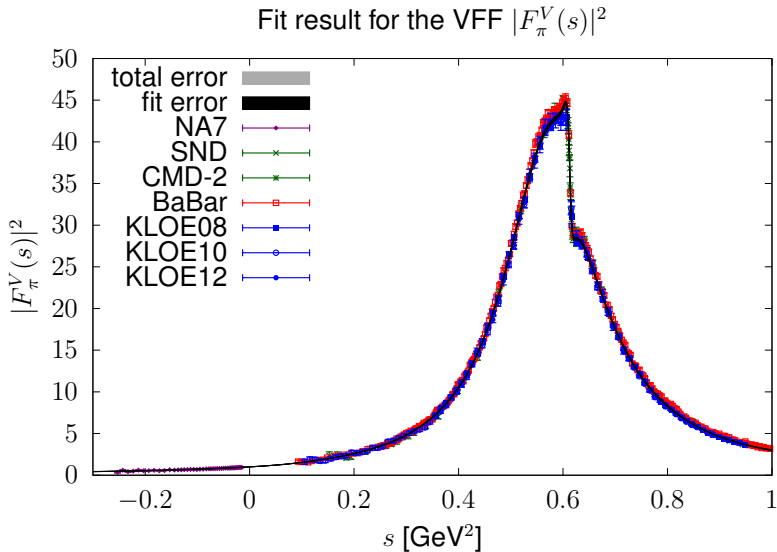
- value of the elastic $\pi\pi$ -scattering P -wave phase shift δ_1^1 at two points (0.8 GeV and 1.15 GeV)
- $\rho - \omega$ mixing parameter ϵ_ω
- ω mass
- energy rescaling for the experimental input, which allows for a calibration uncertainty
- $N - 1$ coefficients in the conformal polynomial

VFF fit to the following data

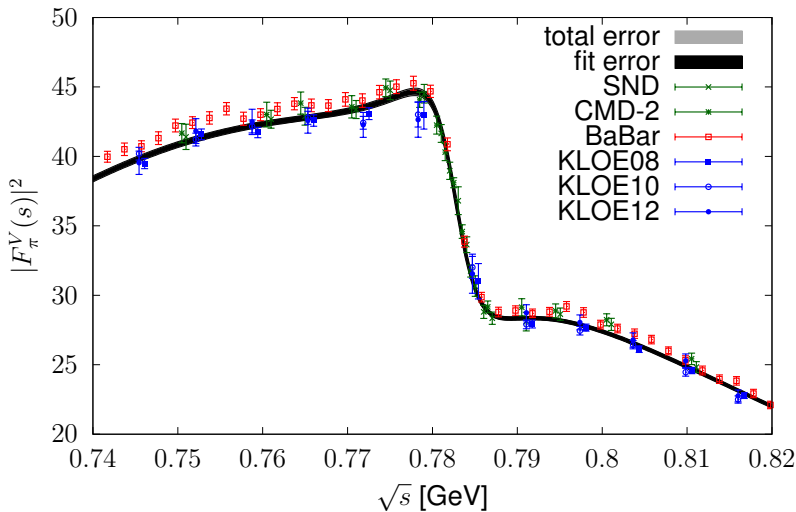
- time-like cross section data from high-statistics e^+e^- experiments SND, CMD-2, BaBar, KLOE
- space-like VFF data from NA7
- Eidelman – Łukaszuk bound on inelastic phase:
→ [Eidelman, Łukaszuk, 2004](#)
- iterative fit routine including full experimental covariance matrices and avoiding D'Agostini bias
→ [D'Agostini, 1994](#); [Ball et al. \(NNPDF\) 2010](#)

VFF fit results

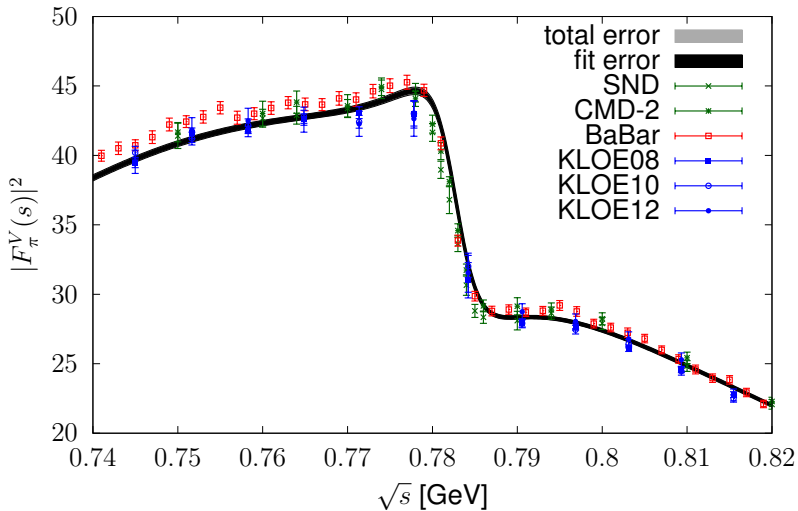
- perfect fits to all experiments possible (p -value around 3% to 6%) with a few caveats:
 - either M_ω or energy recalibration has to be fit (practically identical results)
 - two outliers in KLOE08 set (> 30 units in χ^2)
 - BESIII covariance matrix cannot be used
- well-known discrepancy between BaBar and KLOE
 \Rightarrow fit all data sets and inflate errors by $\sqrt{\chi^2/\text{dof}}$
- inelastic effects dominate uncertainty for $(g - 2)_\mu$

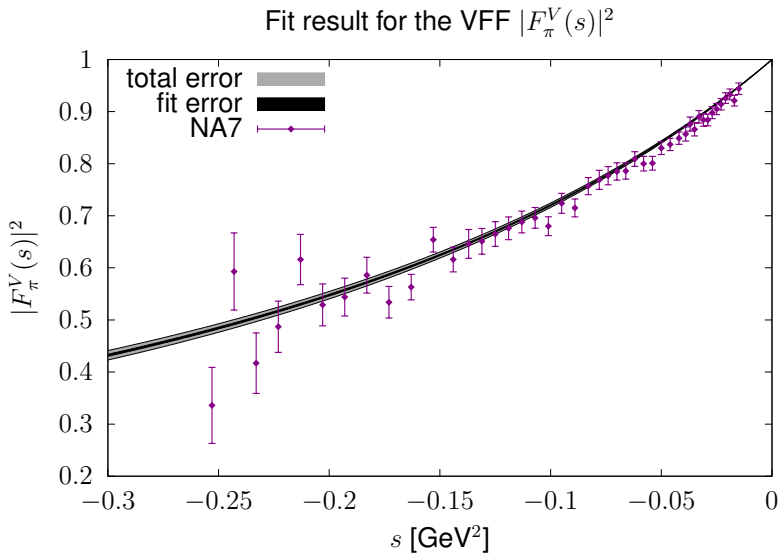


VFF fit result and data with energy rescaling

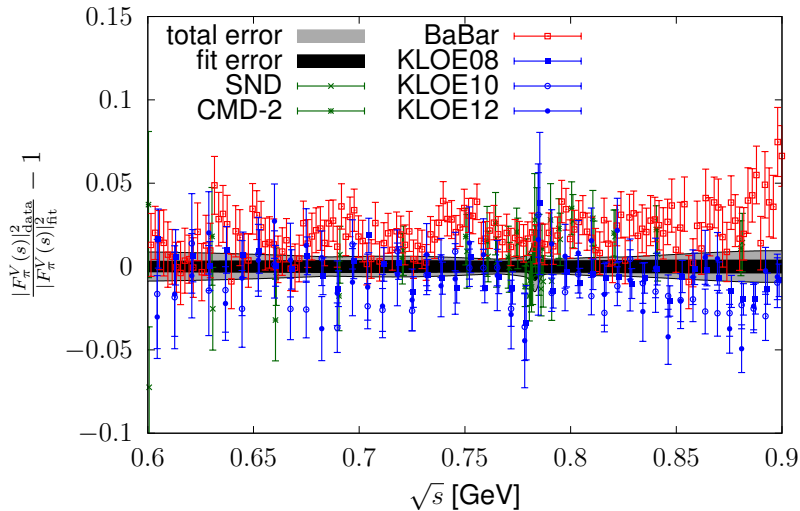


VFF fit result and data without energy rescaling





Relative difference between data sets and fit result



Contribution to $(g - 2)_\mu$

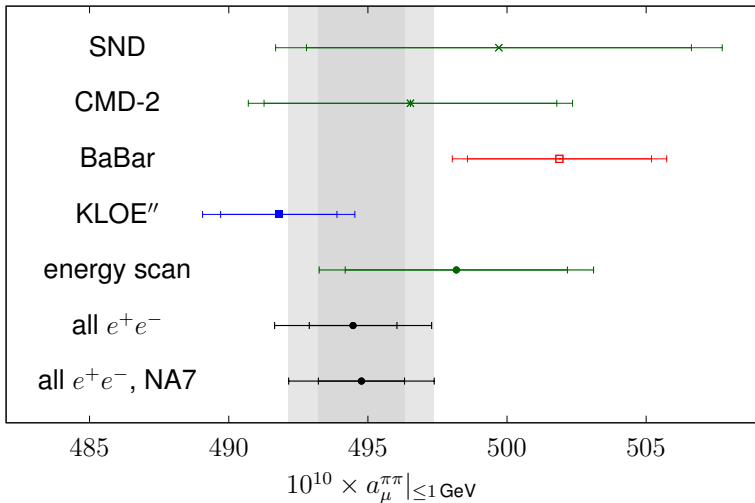
- low-energy $\pi\pi$ contribution:

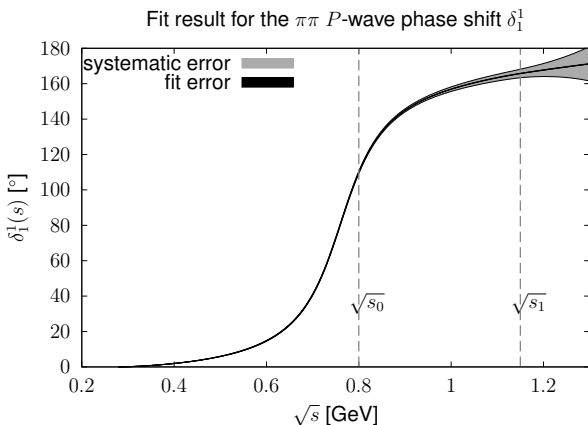
$$a_\mu^{\text{HVP},\pi\pi}|_{\leq 0.63 \text{ GeV}} = 132.8(0.4)(1.1) \times 10^{-10}$$

\Rightarrow compare to 131.1(1.0) \rightarrow [KNT18](#), 133.3(7) \rightarrow [Ananthanarayan et al., 2016](#)

- $\pi\pi$ contribution up to 1 GeV:

$$a_\mu^{\text{HVP},\pi\pi}|_{\leq 1 \text{ GeV}} = 494.8(1.5)(2.1) \times 10^{-10}$$

Result for $a_\mu^{\text{HVP}, \pi\pi}$ below 1 GeV

Improved determination of $\delta_1^1(s)$ 

$$\delta_1^1(s_0) = 110.4(1)(7)^\circ = 110.4(7)^\circ$$

$$\delta_1^1(s_1) = 165.7(0.1)(2.4)^\circ = 165.7(2.4)^\circ$$

Determination of the pion charge radius

definition of charge radius:

$$F_\pi^V(s) = 1 + \frac{1}{6} \langle r_\pi^2 \rangle s + \mathcal{O}(s^2)$$

dispersion relation for F_π^V implies sum rule:

$$\langle r_\pi^2 \rangle = \frac{6}{\pi} \int_{4M_\pi^2}^{\infty} ds \frac{\text{Im} F_\pi^V(s)}{s^2}$$

our result:

$$\langle r_\pi^2 \rangle = 0.429(1)(4) \text{ fm}^2 = 0.429(4) \text{ fm}^2$$

compare to PDG: $\langle r_\pi^2 \rangle = 0.452(11) \text{ fm}^2$

(includes potentially model-dependent $eN \rightarrow e\pi N$)

A puzzle: ω mass

fit result for ω mass:

$$\text{combined fit: } M_\omega = 781.69(9)(3) \text{ MeV}$$

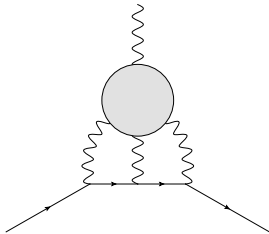
$$\text{fits to single experiments: } M_\omega = 781.49 \dots 782.05 \text{ MeV}$$

compare to PDG value (dominated by 3π channel):

$$M_\omega^{\text{PDG}} = 782.65(12) \text{ MeV}$$

- 1 Hadronic contributions to the muon $g - 2$
- 2 Hadronic vacuum polarisation
- 3 Hadronic light-by-light scattering**
 - Tensor decomposition and Mandelstam representation
 - Pion pole
 - Pion box
 - $\pi\pi$ -rescattering
- 4 Conclusions and outlook

Dispersive approach



- make use of fundamental principles:
 - gauge invariance, crossing symmetry
 - unitarity, analyticity
- relate HLbL to experimentally accessible quantities

BTT Lorentz decomposition

Lorentz decomposition of the HLbL tensor:

→ Bardeen, Tung (1968) and Tarrach (1975)

$$\Pi^{\mu\nu\lambda\sigma}(q_1, q_2, q_3) = \sum_i T_i^{\mu\nu\lambda\sigma} \Pi_i(s, t, u; q_j^2)$$

- Lorentz structures manifestly gauge invariant
- scalar functions Π_i free of kinematic singularities
⇒ dispersion relation in the Mandelstam variables

Dispersive representation

- write down a double-spectral (Mandelstam) representation for the HLbL tensor
- split the HLbL tensor according to the sum over intermediate (on-shell) states in unitarity relations

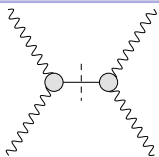
$$\Pi_{\mu\nu\lambda\sigma} = \Pi_{\mu\nu\lambda\sigma}^{\pi^0\text{-pole}} + \Pi_{\mu\nu\lambda\sigma}^{\text{box}} + \Pi_{\mu\nu\lambda\sigma}^{\pi\pi} + \dots$$

Dispersive representation

- write down a double-spectral (Mandelstam) representation for the HLbL tensor
- split the HLbL tensor according to the sum over intermediate (on-shell) states in unitarity relations

$$\Pi_{\mu\nu\lambda\sigma} = \Pi_{\mu\nu\lambda\sigma}^{\pi^0\text{-pole}} + \Pi_{\mu\nu\lambda\sigma}^{\text{box}} + \Pi_{\mu\nu\lambda\sigma}^{\pi\pi} + \dots$$

one-pion intermediate state

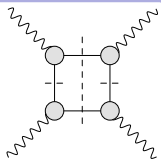


Dispersive representation

- write down a double-spectral (Mandelstam) representation for the HLbL tensor
- split the HLbL tensor according to the sum over intermediate (on-shell) states in unitarity relations

$$\Pi_{\mu\nu\lambda\sigma} = \Pi_{\mu\nu\lambda\sigma}^{\pi^0\text{-pole}} + \Pi_{\mu\nu\lambda\sigma}^{\text{box}} + \Pi_{\mu\nu\lambda\sigma}^{\pi\pi} + \dots$$

two-pion intermediate state in both channels

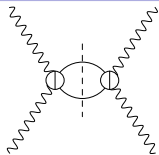


Dispersive representation

- write down a double-spectral (Mandelstam) representation for the HLbL tensor
- split the HLbL tensor according to the sum over intermediate (on-shell) states in unitarity relations

$$\Pi_{\mu\nu\lambda\sigma} = \Pi_{\mu\nu\lambda\sigma}^{\pi^0\text{-pole}} + \Pi_{\mu\nu\lambda\sigma}^{\text{box}} + \Pi_{\mu\nu\lambda\sigma}^{\pi\pi} + \dots$$

two-pion intermediate state in first channel



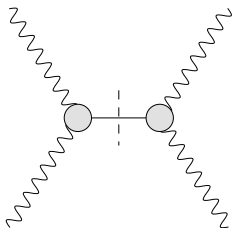
Dispersive representation

- write down a double-spectral (Mandelstam) representation for the HLbL tensor
- split the HLbL tensor according to the sum over intermediate (on-shell) states in unitarity relations

$$\Pi_{\mu\nu\lambda\sigma} = \Pi_{\mu\nu\lambda\sigma}^{\pi^0\text{-pole}} + \Pi_{\mu\nu\lambda\sigma}^{\text{box}} + \Pi_{\mu\nu\lambda\sigma}^{\pi\pi} + \dots$$

higher intermediate states

Pion pole



$$\bar{\Pi}_1^{\pi^0\text{-pole}} = \frac{\mathcal{F}_{\pi^0\gamma^*\gamma^*}(q_1^2, q_2^2)\mathcal{F}_{\pi^0\gamma^*\gamma}(q_3^2, 0)}{q_3^2 - M_\pi^2}$$

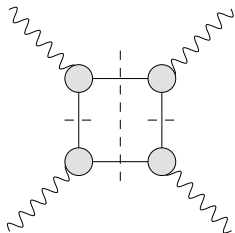
$\bar{\Pi}_2^{\pi^0\text{-pole}}$ via crossing symmetry

- input: doubly-virtual and singly-virtual pion transition form factors $\mathcal{F}_{\gamma^*\gamma^*\pi^0}$ and $\mathcal{F}_{\gamma^*\gamma\pi^0}$
- dispersive analysis of transition form factor:

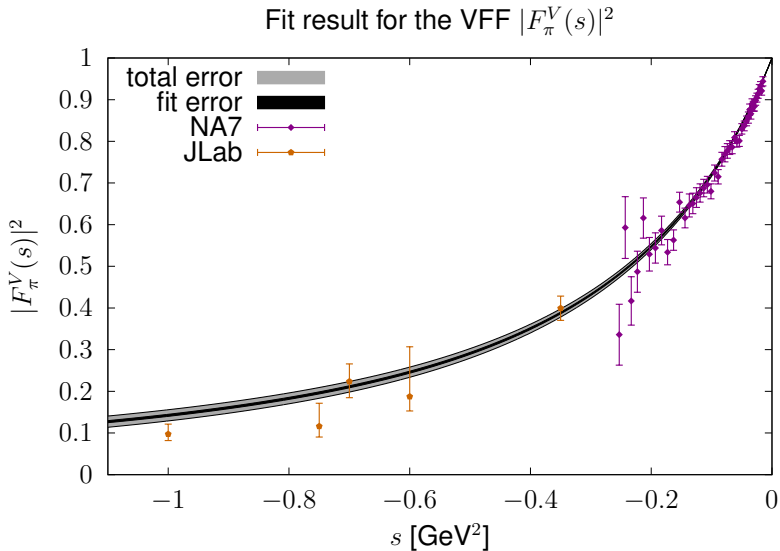
$$a_\mu^{\pi^0\text{-pole}} = 62.6_{-2.5}^{+3.0} \times 10^{-11}$$

→ Hoferichter et al., PRL 121 (2018) 112002, JHEP 10 (2018) 141

Box contribution

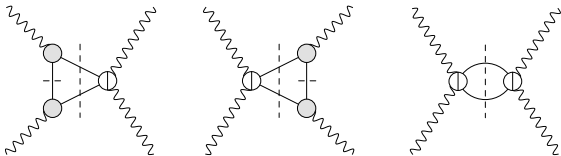


- simultaneous two-pion cuts in two channels
- Mandelstam representation explicitly constructed
- q^2 -dependence: pion VFF $F_\pi^V(q_i^2)$ for each off-shell photon factor out
- Wick rotation: integrate over space-like momenta
- dominated by low energies ≤ 1 GeV
- result: $a_\mu^{\pi\text{-box}} = -15.9(2) \times 10^{-11}$



(the JLab data are not used in the fit)

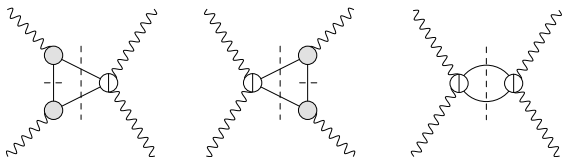
Rescattering contribution



- neglect left-hand cut due to multi-particle intermediate states in crossed channel
- two-pion cut in only one channel:

$$\begin{aligned} \Pi_i^{\pi\pi} = & \frac{1}{2} \left(\frac{1}{\pi} \int_{4M_\pi^2}^{\infty} dt' \frac{\text{Im}\Pi_i^{\pi\pi}(s, t', u')}{t' - t} + \frac{1}{\pi} \int_{4M_\pi^2}^{\infty} du' \frac{\text{Im}\Pi_i^{\pi\pi}(s, t', u')}{u' - u} \right. \\ & + \text{fixed-}t \\ & \left. + \text{fixed-}u \right) \end{aligned}$$

Rescattering contribution



- expansion into partial waves
- unitarity gives imaginary parts in terms of helicity amplitudes for $\gamma^* \gamma^{(*)} \rightarrow \pi\pi$:

$$\text{Im}_{\pi\pi} h_{\lambda_1 \lambda_2, \lambda_3 \lambda_4}^J(s) \propto \sigma_\pi(s) h_{J, \lambda_1 \lambda_2}(s) h_{J, \lambda_3 \lambda_4}^*(s)$$

- framework valid for arbitrary partial waves
- resummation of PW expansion reproduces full result: checked for pion box

S -wave rescattering contribution

- pion-pole approximation to left-hand cut
 $\Rightarrow q^2$ -dependence given by F_π^V
- phase shifts based on modified inverse-amplitude method ($f_0(500)$ parameters accurately reproduced)
- result for S -waves:

$$a_{\mu, J=0}^{\pi\pi, \pi\text{-pole LHC}} = -8(1) \times 10^{-11}$$

- 1 Hadronic contributions to the muon $g - 2$
- 2 Hadronic vacuum polarisation
- 3 Hadronic light-by-light scattering
- 4 Conclusions and outlook**

HVP

- precise dispersive determination of pion VFF
- comprehensive analysis of uncertainties in $\pi\pi$ channel
- valuable to corroborate uncertainties of direct integration methods
- precise prediction for low-energy region, but useful up to 1 GeV:

$$a_{\mu}^{\text{HVP},\pi\pi}|_{\leq 1 \text{ GeV}} = 494.8(1.5)(2.1) \times 10^{-10}$$

- side-products: improved determination of $\pi\pi$ P -wave phase shift; pion charge radius

HLbL

- very precise evaluation of HLbL pion-box contribution:

$$a_{\mu}^{\pi\text{-box}} = -15.9(2) \times 10^{-11}$$

- precise prediction for S -wave $\pi\pi$ -rescattering contribution with pion-pole left-hand cut:

$$a_{\mu, J=0}^{\pi\pi, \pi\text{-pole LHC}} = -8(1) \times 10^{-11}$$

- D -wave contribution work in progress: requires inclusion of higher left-hand cuts
- contributions beyond $\pi\pi$ and pQCD/OPE constraints work in progress

Summary

- our dispersive approach to HVP and HLbL is based on fundamental principles:
 - gauge invariance, crossing symmetry (for HLbL)
 - unitarity, analyticity
- we are focusing on the lightest intermediate states
- relation to experimentally accessible (or again with data dispersively reconstructed) quantities
- precise numerical evaluation of two-pion contributions
- a step towards a model-independent calculation of a_μ